

Degradation rate of DNA scaffolds and bone regeneration

Ayako Matsumoto^{1, 2}, Hiroshi Kajiya^{1, 3*}, Nana Yamamoto-M⁴, Tsukasa Yanagi², Ayaka Imamura¹, Koji Okabe³, Tadao Fukushima^{1#}, Hirofumi Kido² and Jun Ohno¹

¹Research Center for Regenerative Medicine, Fukuoka Dental College, 2-15-1 Tamura, Fukuoka, Japan

²Department of Oral Rehabilitation, Fukuoka Dental College, 2-15-1 Tamura, Fukuoka, Japan

³Department of Physiological Science and Molecular Biology, Fukuoka Dental College, 2-15-1 Tamura, Fukuoka, Japan

⁴ Department of Odontology, Fukuoka Dental College, 2-15-1 Tamura, Fukuoka, Japan

This author is a retired professor.

*Corresponding author: kajiya@college.fdcnet.ac.jp

Department of Physiological Science and Molecular Biology, Fukuoka Dental College, Fukuoka, 8140193 Japan

Running head: Degradation rate and bone regeneration

Abstract (195 words)

Scaffolds implanted into bone defect sites must achieve optimal biodegradation rates while appropriately filling the void as new bone formation progresses. We recently developed a unique biomaterial comprising a mix of salmon DNA and protamine that can be used as an osteoconductive scaffold for tissue engineering. The aim of the present study was to elucidate how the degradation rate of the scaffold affects bone regeneration. We examined the relationships between the degradation rate using salmon DNA scaffolds and new bone formation using a rat skin flank subcutaneous model and a rat calvarial defect model. The degradation rate of the scaffolds was proportional to the duration of pretreatment with UV irradiation, with degradation rates proportional to the duration of irradiation. Scaffolds irradiated with UV for 0.5 h maintained a gradual degradation of phosphate as compared with scaffolds irradiated for 0 or 3.0 h, as tested in a subcutaneous tissue implantation model. In the calvarial defect model, we found that new bone formation was higher in rats treated with UV irr (0.5) scaffolds as compared with UV irr (0) and UV irr (3.0) scaffolds. The present results suggest that bioengineering of scaffold biodegradation is an important to bone regeneration.

Key words: bone regeneration, scaffold, phosphate, biodegradation, calvarial defect

INTRODUCTION

DNA has suitable biocompatibility for integration with biomaterials for drug delivery systems [1-5], as it can intercalate and bind antibiotics or proteins between stacked base pairs or within grooves [1, 2]. In particular, in bone tissue engineering, the phosphate groups of DNA could be relevant, as phosphate is known to upregulate osteopontin expression and enhance mineralization in vitro [6-8]. Indeed, some reports have demonstrated osteogenesis in response to DNA-based biomaterials; for example, titanium coated with DNA can increase the differentiation of osteoblast-like cells and the deposition of osteocalcin, an important matrix protein involved in tissue mineralization [9]. Furthermore, we previously showed that a DNA/protamine complex can induce new bone formation in a rat calvarial defect model [10-12]. DNA degradation releases phosphate ions that bear a strong affinity for calcium ions, producing calcium phosphate, an important bone matrix constituent. Some reports have indicated that the extracellular phosphate promotes osteogenic differentiation and calcification of preosteoblasts [13, 14] and mesenchymal stem cells [15, 16]. Furthermore, we have recently shown that the DNA itself can enhance osteogenesis via the upregulation of a phosphate transporter activity and cell migration [17, 18], resulting in new bone formation in a calvarial defect model.

Scaffolding materials for tissue engineering are typically also designed to provide a space or support structure for migrating and infiltrating cells to attach, proliferate, and produce new extracellular matrix [19, 20]. In bone tissue engineering, the deposition and mineralization of

bone matrix are required for bone development and repair, and the use of osteoconductive or osteoinductive scaffolding materials, functionalized with appropriate proteins or drugs, can aid in this process [21]. As the new bone is formed, the scaffold must then degrade to allow the new bone matrix to replace the scaffold and properly integrate with the existing bone [22, 23]. However, the rate of biodegradation is presumed to have a profound effect on the success of the repair, as degradation that is too fast would fail to support the repair site, and degradation that is too slow would also hinder appropriate tissue replacement and integration with the existing bone [24]. However, as yet, there is little direct evidence to support a relation between the biodegradation rate of the scaffold and the quantity and quality of an engineered tissue *in vivo*.

This study sought to address the hypothesis that modifying the degradation rate of a DNA scaffold using UV light irradiation would directly control the extent of new bone formation. We used our previously established salmon DNA scaffold and variable duration of UV irradiation to test our hypothesis in a rat skin flank subcutaneous model and a rat calvarial bone defect model.

MATERIALS AND METHODS

Preparation of DNA discs

Salmon testis DNA (more than 20,000 bp DNA; Maruha-Nichiro Corporation, Tokyo, Japan) was precipitated with ethanol, and then mixed with distilled water to prepare a jelly-like paste. The molecular weight of the DNA was confirmed using electrophoresis analysis [12]. We first tested various concentrations of DNA (50, 100, and 150 mg/ml) to create the appropriate “DNA paste” consistency (Fig. 1A). The change in the diameter of DNA paste was measured until 48 h under a humid environment. The DNA paste at a concentration of 100 mg/ml maintained its shape over time, whereas the diameter increased for 50 mg/ml and decreased for 150 mg/ml. As a result, we used 100 mg/ml as our final concentration.

To prepare the scaffold for implantation, the DNA paste was injected into a silicone mold (internal diameter, 8 mm; height, 0.8 mm) on a polytetrafluoroethylene plate, and frozen with liquid nitrogen [12, 17, 18]. The fabricated DNA discs were immediately and carefully removed from the silicon mold and plate and dried for 24 h in a FD-5N freeze-dryer. To modify the degradation rate of the DNA discs they were fixed 1cm from an apparatus UV light irradiator (U type UV ramp kit, Sun Energy Co. Ltd., Osaka, Japan.) and subjected to continuous UV irradiation (condition; wave length; 254 nm, intensity; 10mW/cm²) for 0 , 0.25, 0.5, 1.0, 3.0 and 5.0 h. The DNA discs were sterilized using gamma-ray irradiation .

DNA disc degradation rate in water

To measure disc degradation rates, the discs were continuously immersed in 10 ml of

distilled water and coupled with 10cm culture dish at 25°C using incubator. The eluting solution was filtered and collected over a time frame of 48 h. The absorbance in the eluted solution was scanned with a V-560 spectrophotometer (range, 200 to 300 nm; Jasco Corp., Tokyo, Japan). The amount of degraded DNA was calculated from the difference in the total peak area between each eluting solution and each standard solution.

Disc structure observation using field emission-scanning electron microscopy (FE-SEM)

DNA discs with or without UV irradiation were freeze-fractured to observe the surface structures. The fractured surfaces were coated with evaporated carbon on a planetary rotating stage followed by sputter coating with a 20 nm layer of platinum (Polaron E5150 Sputter Coater). An accelerating voltage of 0.5 kV was chosen for FE-SEM analysis using a JSM-6330F FE-SEM (JEOL, Tokyo, Japan) and the micrographs were captured using secondary electrons collected with an in-lens detector.

Compression test in discs

To test the mechanical property in UV irradiated and non-irradiated DNA discs ten piled DNA discs were uniaxially compressed when the loading weight was changed from 2 to 30g. The DNA discs were held using cylinder to prevent any lateral movement. The vertical heights of DNA discs immersed in PBS were measured by travelling microscope (Manufacturer: SHIMADZU, TypeA, No101794, Japan).

Implantation of DNA discs in Calvarial defect models

Animal experiments were performed in accordance with the ethical guidelines for animal experiments at Fukuoka Dental College (No. 13009). Ten-week-old male Sprague-Dawley rats (weight of approximately 350g) or 10-weeks-old mice were used in the present study. Surgery was carried out under anesthesia using 2% isoflurane (Abbott Laboratories, Abbott Park, IL, USA) and an air mixture gas flow of 1.0 L/min using an anesthesia gas machine (Anesthesia machine SF-B01; MR Technology, Inc., Tsukuba, Ibaraki, Japan). An incision was made in the skin of the cranium, and the periosteum was exposed, incised in a semicircle, and carefully detached from the cranial bone. Eight-millimeter calvarial defects were created in the exposed central parietal bone using a trephine drill. Defects with sham treatment were used as controls. The DNA discs (diameter, 8mm) were inserted and the periosteum and cranial tissues were closed in layers. Five rats were sacrificed at each 2, 4, 8, and 12 weeks to measure new bone formation.

Implantation of DNA disk in subcutaneous back flap

To confirm the biocompatibility and biodegradability of the DNA discs with or without UV irradiation, UV irradiated (UV irr (0.5) and UV irr (3.0)) and non-irradiated (UV irr (0)) discs were implanted subcutaneously on the backs of rats [12]. The soft tissues were closed in separate layers by suturing. The controls consisted of a group of sham-operated rats without sample implantation. Samples were harvested on days 1, 3, 7, and 14 after implantation using subcutaneous back flap experiments ($n = 5$ from each group at each time point)

Micro-computed tomography (CT) analyses

Micro-CT images were taken using in vivo μ -CT equipment (Skyscan-1176; Bruker, Belgium) at 50 kV and 500 μ A. Each μ -CT slice was 18 μ m thick. After scaffold materials transiently provide a space and/or support structure during osteogenesis bone healing have reported to require for 3-6 months [17, 18]. Then, samples were harvested on 2, 4, 8, and 12 weeks after implantation using cranial implant experiments ($n = 5$ from each group at each time point). New bone formation in the defect area was obtained from each μ -CT image and calculated as the percentage of newly formed bone within the area of the original defect created by trephination, as previously described [10]. Newly formed bone in the horizontal direction was first quantified two-dimensionally using WINROOF image analysis software (Mitani Corp., Tokyo, Japan). Then, 8-mm diameter circles were drawn on each μ -CT slice image for analysis. A series of ten μ -CT images, showing areas of the highest amount of new bone formation, were used for each sample analysis. The percentage of new bone formation in the defect (% of new bone) was calculated as the total area of new bone formation per 10 μ -CT slice images $\times 100$.

Hematoxylin and eosin (HE) staining

Rodent calvariae were collected on 4, 8, and 12 weeks. The samples were fixed in 4% (w/v) paraformaldehyde in phosphate buffer (pH 7.4), decalcified with 0.24 M EDTA \cdot 4Na \cdot 4H₂O solution, dehydrated with graded alcohols, cleared in xylene, and embedded in paraffin.

Staining was performed on 3- μ m-thick sections by routine procedures. The paraffin sections were stained with hematoxylin and eosin (HE) to evaluate any histological changes, All sections were histologically observed with a Nikon Eclipse Ti-u fluorescence microscope (Nikon, Tokyo, Japan).

Phosphate concentration measurements

The level of phosphates released into the culture medium was determined by use of Phosphor C a phosphate assay kit (Wako, Osaka, Japan) according to the manufacturer's recommended protocol at each time point. Briefly, DNA discs with or without UV irradiation were placed in the upper chambers of cell culture well inserts (8- μ m pore size; PET track-etched membrane) and incubated in α -MEM with 10% FBS for 0, 1, 3, 6, 24, 48 and 72 h at 37°C.

Statistical analysis

Data are expressed as the mean \pm standard error of the mean (SEM). Statistical comparisons were made using the Mann-Whitney U-test. A *P* value < 0.05 was considered statistically significant.

RESULTS

Properties of UV irradiated and nonirradiated salmon DNA discs

Some reports have been shown that the UV irradiation induced the formation of thymine-thymine dimer structure [25, 26, 27]. The UV-irradiated salmon DNA firm was water-insoluble and showed resistance to hydrolysis by nuclease compared to non-irradiated DNA firm,

suggesting the formation of DNA intermolecular crosslinking with a three-dimensional network [27]. The surfaces of all DNA discs were porous (diameter, 10-30 μm) (FE-SEM; Fig. 1B), with the size and shape of the pores similar between irradiated and non-irradiated discs. To clarify the relationship between degradation rate and UV irradiation in DNA discs, we collected and measured the amount of eluted DNA after the UV-irradiated and non-irradiated discs were immersed in water for 48 h (Fig. 1C). As expected, we found a gradual increase in the amount of degraded DNA in the water in a time-dependent manner, with a peak at 25 h. Degradation was slower for the UV-irradiated discs than the non-irradiated discs. Among the used irradiated and non-irradiated DNA discs, UV irr (0) and UV irr (0.25), UV irr (0.5) and UV irr (1.0), and UV irr (3.0) and UV irr (5.0) showed similar in degradation time-course. Therefore, UV irr (0), UV irr (0.5) and UV irr (3.0) were used in the following experiments. Furthermore, to evaluate mechanical properties in irradiated and non-irradiated DNA discs we were compressed them loaded with weight (Fig. 1D). We found a gradual decrease in the change in compressed length in a weight-dependent manner. The change in compressed length was smaller for the UV-irradiated discs than the non-irradiated discs, suggesting in the UV-irradiated new intermolecular formation.

Effect of UV irradiation on biodegradability of DNA disc

We next evaluated the biocompatibility and biodegradability in UV irradiated and non-irradiated DNA discs inserted subcutaneously into the flanks of Sprague-Dawley rats (Fig. 2).

On day 1 after implantation, all discs were surrounded by band-like inflated neutrophils regardless of the pretreatment with or without UV irradiation, with no evidence of bacterial colonies in the surrounding tissues. On day 5, implanted non-irradiated discs had been completely degraded and replaced by inflammatory granulation tissue containing numerous lymphocytes and several plasma cells. However, on day 5 both irradiated discs fractionated with smaller and thinner. The non-degraded materials were remained to the periphery of implanted site, which was circumscribed by cellular granulation tissues. No foreign-body giant cells were observed in the granulation tissue. On day 7, the cellular granulation tissue in the implant sites had been replaced by a fibrous connective tissue containing a few inflammatory cells and vascular slits. DNA discs irradiated for 0.5 h were almost absorbed on day 7, and the implanted sites showed dilated, empty spaces surrounded by granulation tissue. On contrast, DNA disc irradiated for 3h remained a little non-biograduated materials on day 14.

These results indicate that discs treated for longer with UV irradiation showed slower biodegradation, and suggests that a giant cell-independent foreign-body reaction contributes to the biodegradation.

Implantation of UV-irradiated DNA discs promote calvarial bone regeneration

To clarify whether UV-irradiated DNA discs can potentiate regeneration better than non-treated discs, we implanted DNA discs into calvarial bone defects in 10-week-old Sprague-Dawley rats (Fig. 3). Previous reports suggest that calvarial defects in Sprague-Dawley rats do not heal

spontaneously during the bone regeneration period [28]. We used micro-CT scanning to assess calvarial bone regeneration. At 2 weeks after surgery, we observed small peninsulas of new bone formation in the rats implanted with the discs, with higher rates noted in the rats implanted with UV irr (0.5) DNA discs as compared with rats in the sham, UV irr (0), and UV irr (3.0) groups. This trend continued up to 12 weeks. These results were confirmed by histological analysis of HE-stained sections at 12 weeks, with evidence of new bone regeneration in rats treated with the UV irr (0.5) discs. However, in both non- and irradiated discs, active osteoblast-like cells were found lining the periphery of the newly formed calvarial bone. These findings indicate that irradiated DNA discs can promote bone regeneration in rat calvarial defects better than non-irradiated discs. Similar results were obtained using a mouse calvarial defect model (Supplemental Fig.1).

UV irr (0.5) DNA discs continuously release phosphate

To clarify why UV irr (0.5) DNA discs showed better bone promoting effects, we examined the net rate of DNA degradation into phosphate using a transwell culture method (Fig. 4). In the absence of discs, the phosphate concentrations remained almost constant in both the upper chamber and lower well of the assay. On 1 h after placement of DNA discs, the phosphate concentration in lower wells slightly decreased in the three types of discs, suggesting that they absorbed and swelled with the culture medium. Furthermore, the UV irr (0) DNA disc released few permeable phosphate ions from 3 h to 48 h after incubation. Comparatively, placing the

DNA irr (0.5) and (3.0) discs in the upper chamber increased the phosphate concentration in the lower well in a time-dependent manner. Intriguingly, the UV irr (0.5) DNA disc continuously released permeable phosphate ions from 3 h to 48 h after incubation as compared with the UV irr (0) and UV irr (3.0) discs. The UV irr (3.0) disc transiently increased phosphate ions on the 48 h.

DISCUSSION

The present experiments show that the degradation rates of DNA discs influences the rate of bone formation. Non-irradiated DNA discs degraded quickly, resulting in a limited amount of new bone formation. However, UV-irradiated discs, bearing crosslinked nuclear acids, degraded slower, and we hypothesize that the slower release of phosphate ions improved the rates of bone formation in the defect site. These results support that the rates of degradation of biomaterials can change the production and integration of new bone tissues at sites of repair.

The irradiated DNA discs in the present study were less susceptible to biodegradation than the non-treated DNA discs, with the rate of degradation dependent on the duration of UV pretreatment. The biodegradation process of implanted materials is composed of two phases: 1) the humoral phase, which is mediated the extracellular enzymes secreted from the blood plasma and the surrounding tissues; and 2) the cellular phase, which is activated by phagocytes and foreign-body giant cells [29]. Here, we found that UV irradiation led to slower biodegradation rates and dissolution rates, both of which were dependent on the duration of UV pretreatment.

Furthermore, we found that the degradation process of implanted non-treated discs did not require phagocytic activity. Thus, DNase secreted from the surrounding tissues contributes to the degradation of the non-irradiated DNA disc in the subcutaneous tissue explants. Fibrous connective tissue that is produced alongside biodegradation may adequately fill the bone defect. In contrast, the UV-irradiated DNA discs are degraded by not only extracellular enzymes but also phagocytic activity in the tissue surrounding the discs. We suggest that the differences in the biodegradation processes between the UV-treated and -non-treated discs arose because of phagocytic activity, not sensitivity of the extracellular enzymes. Enzymes that mediate degradation depend on the bioactivity of the disc, because there are no phagocytes in the defect area. Our results indicate that basal levels of phagocytic activity are weak, but are activated on the surfaces of the UV-treated discs.

The dissolution of linear polymers in organic solvents or water is dependent on the polymer molecular weight. We previously reported that 300-bp DNA/protamine scaffolds disappear early after implantation into rat calvarial bone defects [10]. We also showed that high molecular weight DNA—as used in the present experiments—promotes new bone formation by attracting osteoblasts [18]. The addition of DNA into preosteoblast cultures can promote osteogenic differentiation and cellular migration *in vitro*. Thus, we presume that high molecular weight DNA persists until the early stages of bone formation in rat calvarial bone defects. Thus, we sought to determine whether UV irradiation could help to reduce the degradation rates of high

molecular weight DNA discs to facilitate new bone regeneration.

In the calvarial defect model, we found that UV-irradiated discs promoted efficient bone regeneration as compared with the non-irradiated discs using micro-CT analysis. We show that the calvarial bone defects were replaced by extensions of new bone from the defect edges. The DNA discs are thought to be responsible for this bony induction, because the new bone extensions from the defect edges are typical of patterns of bone healing. These findings are consistent with our reports that suggest that the addition of DNA promotes osteogenic differentiation via the direct effect of phosphate ion release from the DNA discs [17]. The concentration of released phosphate is calculated of two factors: 1) the initial step: to dissolve DNA in water 2) the second step: to degraded by enzymes such as DNase and then release phosphate in water. The peak in concentration of phosphates is suggesting to be depended on total time among dissociation, degradation, and releasing and it is different in each type of UV irradiation time. Indeed, in the current study, the UV irr (0.5) DNA discs continuously released phosphate ions in the in vitro assay, suggesting their effectiveness in bone regeneration.

The present study also suggests that a UV-irradiated DNA scaffold may be a critical tissue engineering matrix parameter for better tissue formation and integration. Controlling both the degradation in vitro and in vivo using UV irradiation may offer a powerful tool in the regulation of various regeneration processes across a broad range of tissues. The appropriate degradation rate of a biomaterial will likely affect the migratory activity of different cell types

and perhaps offer a specific strategy for the repair of calvarial defects.

CONCLUSION

In conclusion, our data highlight the osteogenic potential of DNA discs as a strategy for bone repair. DNA exhibits favorable tissue compatibility and biodegradability, releasing phosphate ions into the surrounding tissues. Through controlling the duration of UV irradiation, the degradation rates of DNA discs can be controlled to allow the appropriate time for bone healing.

ACKNOWLEDGMENTS

This work was supported by Grants-in-Aid for Scientific Research from the Ministry of Education, Culture, Sports, Science and Technology of Japan (Nos. 15K11062 to HK, and 15K20420 to NM-Y). We would like to thank the Maruha-Nichiro Corporation for providing the salmon DNA.

DECLARATION

The authors declare no potential conflicts of interest with respect to the authorship and/or publication of this article.

REFERENCES

1. Fukushima T, Kawaguchi M, Hayakawa T, Ohno J, Iwahashi T, Taniguchi K, Inoue Y, Takeda S. Complexation of DNA with cationic polyamino acid for biomaterial purposes. *J Oral Tissue Eng* 2008;6:24-32.
2. Fukushima T, Ohno J, Hayakawa T, Imayoshi R, Mori N, Sakagami R, Mitarai M.

- DNA/protamine complex paste for an injectable dental material. *J Mater Sci Mater Med* 2011;22:2607-2615.
3. van den Beucken JJ, Vos MR, Thüne PC, Hayakawa T, Fukushima T, Okahata Y, Walboomers XF, Sommerdijk NA, Nolte RJ, Jansen JA. Fabrication, characterization, and biological assessment of multilayered DNA-coatings for biomaterial purposes. *Biomaterials* 2006;27:691–701.
 4. Litman RM. A deoxyribonucleic acid polymerase from *Micrococcus luteus* (*Micrococcus lysodeikticus*) isolated on deoxyribonucleic acid-cellulose. *J Biol Chem* 1968;10:243:6222-6233.
 5. Shen X, Nagai N, Murata M, Nishimura D, Sugi M, Munekata M. Development of salmon milt DNA/salmon collagen composite for wound dressing. *J mater Sci: Mater Med* 2008;19:3473-3479.
 6. Fatherazi S, Matsa-Dunn D, Foster BL, Rutherford RB, Somerman MJ, Presland RB. Phosphate regulates osteopontin gene transcription. *J Dent Res* 2009;88:39-44.
 7. Foster BL, Nociti FH Jr, Swanson EC, Matsa-Dunn D, Berry JE, Cupp CJ, Zhang P, Somerman MJ. Regulation of cementoblast gene expression by inorganic phosphate in vitro. *Calcif Tissue Int* 2006;78:103–112.
 8. Langenbach F, Handschel J. Effects of dexamethasone, ascorbic acid and β -glycerophosphate on the osteogenic differentiation of stem cells in vitro. *Langenbach and*

- Handschel Stem Cell Research and Therapy 2013;4:117.
9. van den Beucken JJ, Walboomers XF, Vos MR, Sommerdijk NA, Nolte RJ, Jansen JA. Cyto- and histocompatibility of multilayered DNA-coatings on titanium.
J Biomed Mater Res 2006;77A: 202–211.
 10. Shinozaki Y, Toda M, Ohno J, Kawaguchi M, Kido H, Fukushima T. Evaluation of bone formation guided by DNA/protamine complex with FGF-2 in an adult rat calvarial defect model. J Biomed Mater Res B Appl Biomater 2014;102:1669-1676.
 11. Toda M, Ohno J, Shinozaki Y, Ozaki M, Fukushima T. Osteogenic potential for replacing cells in rat cranial defects implanted with a DNA/protamine complex paste. Bone 2014;67:237-645.
 12. Mori N, Ohno J, Sakagami R, Hayakawa T, Fukushima T. Cell viabilities and biodegradation rates of DNA/protamine complexes with two different molecular weights of DNA. J Biomed Mater Res B Appl Biomater 2013;101:743-751.
 13. Lundquist P, Murer H, Biber J. Type II Na⁺-Pi Cotransporters in Osteoblast Mineral Formation: Regulation by Inorganic Phosphate. Cell Physiol Biochem 2007;19:43-56.
 14. Beck GR Jr, Zerler B, Moran E. Phosphate is a specific signal for induction of osteopontin gene expression. Proc Natl Acad Sci USA 2000;97:8352–8357.
 15. Tsai MT, Li WJ, Tuan RS, Chang WH. Modulation of osteogenesis in human mesenchymal stem cells by specific pulsed electromagnetic field stimulation.

- J Orthop Res 2009;27: 1169–1174.
16. Shih YR, Hwang Y, Phadke A, Kang H, Hwang NS, Caro EJ, Nguyen S, Siu M, Theodorakis EA, Gianneschi NC, Vecchio KS, Chien S, Lee OK, Varghese S. Calcium phosphate-bearing matrices induce osteogenic differentiation of stem cells through adenosine signaling. Proc Natl Acad Sci USA 2014;111:990–995.
17. Katsumata Y, Kajiya H, Okabe K, Fukushima T, Ikebe T. A salmon DNA scaffold promotes osteogenesis through activation of sodium-dependent phosphate cotransporters. Biochem Biophys Res Commun 2015;25:622-628.
18. Sato A, Kajiya H, Mori N, Sato H, Fukushima T, Kido H, Ohno J. Salmon DNA accelerates bone regeneration by inducing osteoblast migration. PloS one 2017;12:e0169522.
19. Putnam AJ, Mooney DJ. Tissue engineering using synthetic extracellular matrices. Nat Med 1996;2:824-826.
20. Alsberg E, Kong JH, Hirano Y, Smith KM, Albeiruti A, Mooney JD. Regulating bone formation via controlled scaffold degradation. J Dent Res 2003;82:903-908.
21. Alsberg E., Hill E.E, Mooney D.J. Craniofacial Tissue Engineering. Crit Rev Oral Biol 2001;2:64-75.
22. Nerem RM, Sambanis A. Tissue engineering: from biology to biological substitutes.

- Tissue Eng 1995;1:3-13.
23. Pollok JM, Vacanti JP. Tissue engineering. *Semin Pediatr Surg* 1996;5:191-196.
24. Bryant SJ, Anseth KS. Hydrogel properties influence ECM production by chondrocytes photoencapsulated in poly (ethylene glycol) hydrogels. *J Biomed Mater Res* 2002;59:63-72.
25. Beukers R. The effect of proflavine on U.V.-induced dimerization of thymine in DNA. *Photochem Photobiol.* 1965;4:935-937.
26. Glisin VR, Doty P. The cross-linking of DNA by ultraviolet radiation. *Biochim Biophys Acta.* 1967; 142:314-322.
27. Yamada M, Kato K, Nomizu M, Sakairi N, Ohkawa K, Yamamoto H, Nishi N. Preparation and characterization of DNA films induced by UV irradiation. *Chemistry.* 2002;8:1407-1412.
28. Schmitz JP, Hollinger JO. The critical size defect as an experimental model for craniomandibulofacial nonunions. *Clin Orthop Relat Res* 1986;205:299-308.
29. von Arx T, Broggini N, Jensen SS, Bornstein MM, Schenk RK, Buser D. Membrane durability and tissue response of different bioresorbable barrier membranes: a histological study in the rabbit calvarium. *Int J Oral Maxillofac Implants* 2005;20: 843-853.

FIGURE LEGENDS

FIGURE 1. Physical properties of UV-irradiated and non-irradiated salmon DNA discs.

(A) Change in diameter of DNA pastes prepared from various DNA concentrations. Data are means \pm SEM from independent 5 samples. $*P < 0.05$ vs 0h. (B) SEM images of DNA discs treated with or without UV irradiation. Scale bar represents 10 μm . (C) Time course of degradation rate of DNA discs immersed in water. Data are means \pm SEM from independent 5 samples. $*P < 0.05$, $**P < 0.01$ vs vs UV irr (0) (D) Change of compressed length to lording weight. Data are means \pm SEM from independent 5 samples. $*P < 0.05$, $**P < 0.01$ vs vs UV irr (0)

FIGURE 2. Time course of histopathology in subcutaneous tissues implanted with DNA

disc with or without UV irradiation. Representative histopathological images show the biodegradation of DNA discs treated with or without UV irradiation in subcutaneous tissues of rat skin. Paraffin sections were stained with a hematoxylin and eosin. Arrow heads indicate the implanted DNA discs. Scale bar represents 500 μm . Similar results were obtained in two independent experiments in the present data.

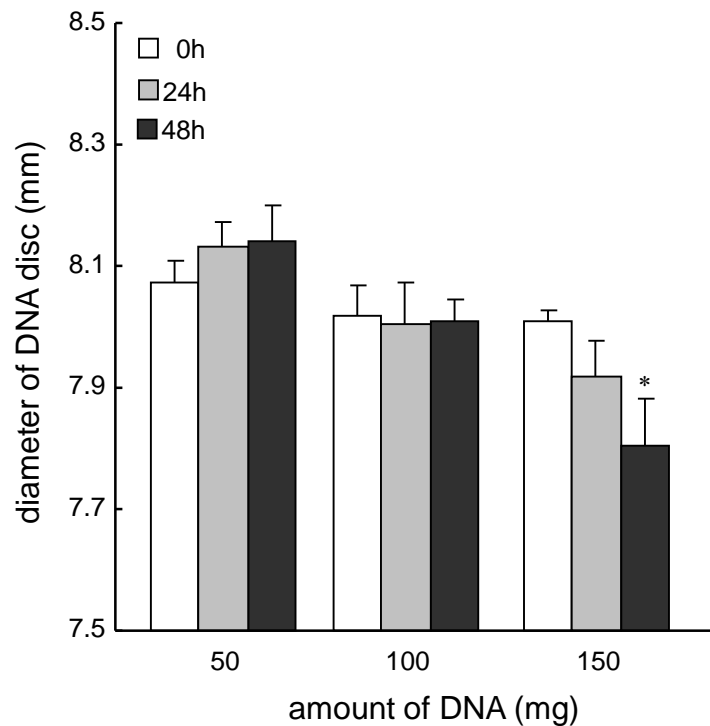
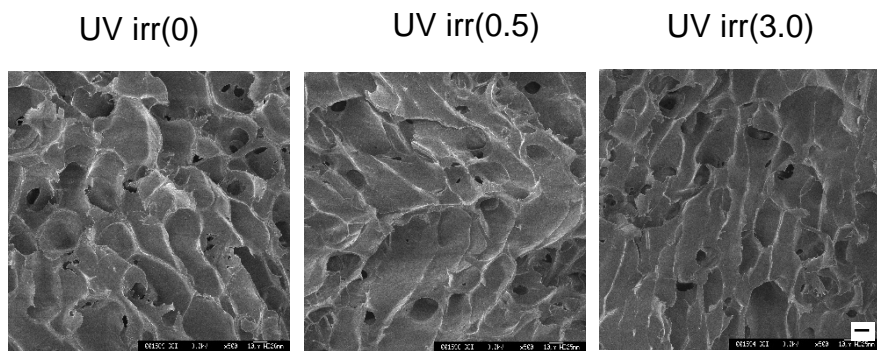
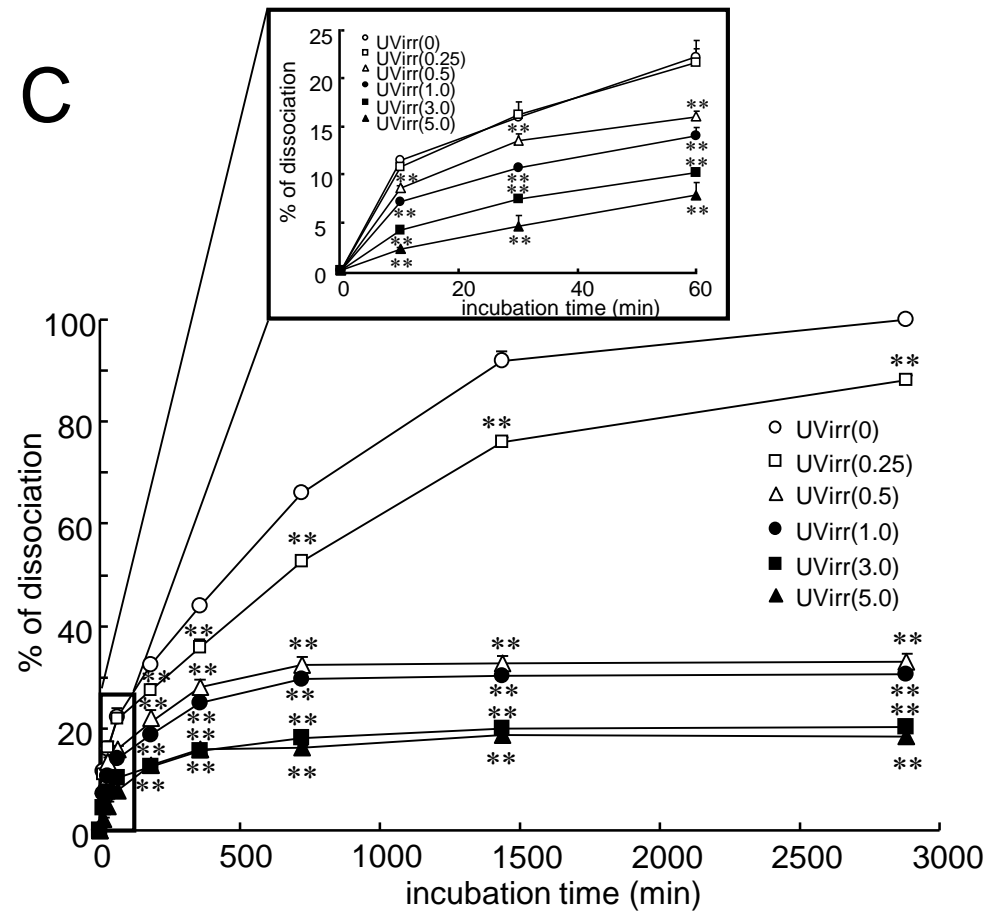
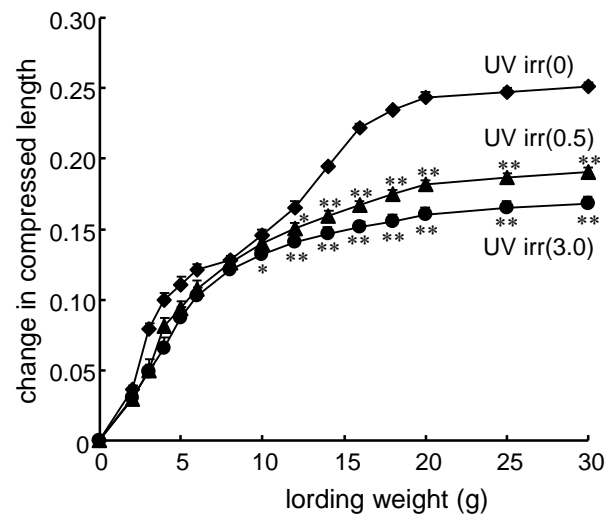
FIGURE 3. Calvarial bone regeneration after implantation of UV irradiated DNA discs.

(A) Calvarial healing at different time points using micro-CT analysis. Procedures for calvarial defects included no treatment (Blank) or treatment with DNA discs pre-treated with or without UV irradiation. (b) Calculation of new bone formation at 2, 4, 8 and 12 weeks after implantation.

The percentage of bone formation was calculated from five rats. Data are shown as the mean and SEM from 5 rats. * $P < 0.05$, ** $P < 0.01$ vs Blank (C) Histological images of calvarial tissues at 12 weeks after surgery. B and N indicate original bone and new bone, respectively; C indicates connective tissues. Scale bar represents 500 μm .

FIGURE 4. Phosphate release from DNA discs with or without UV irradiation.

The phosphate concentration was measured in the collected media in the lower well of the transwell chamber. Data are means \pm SEM from independent 7 wells. * $P < 0.05$ vs UV irr (0)

A**B****Fig.1****C****D**

UV irradiation time (h)

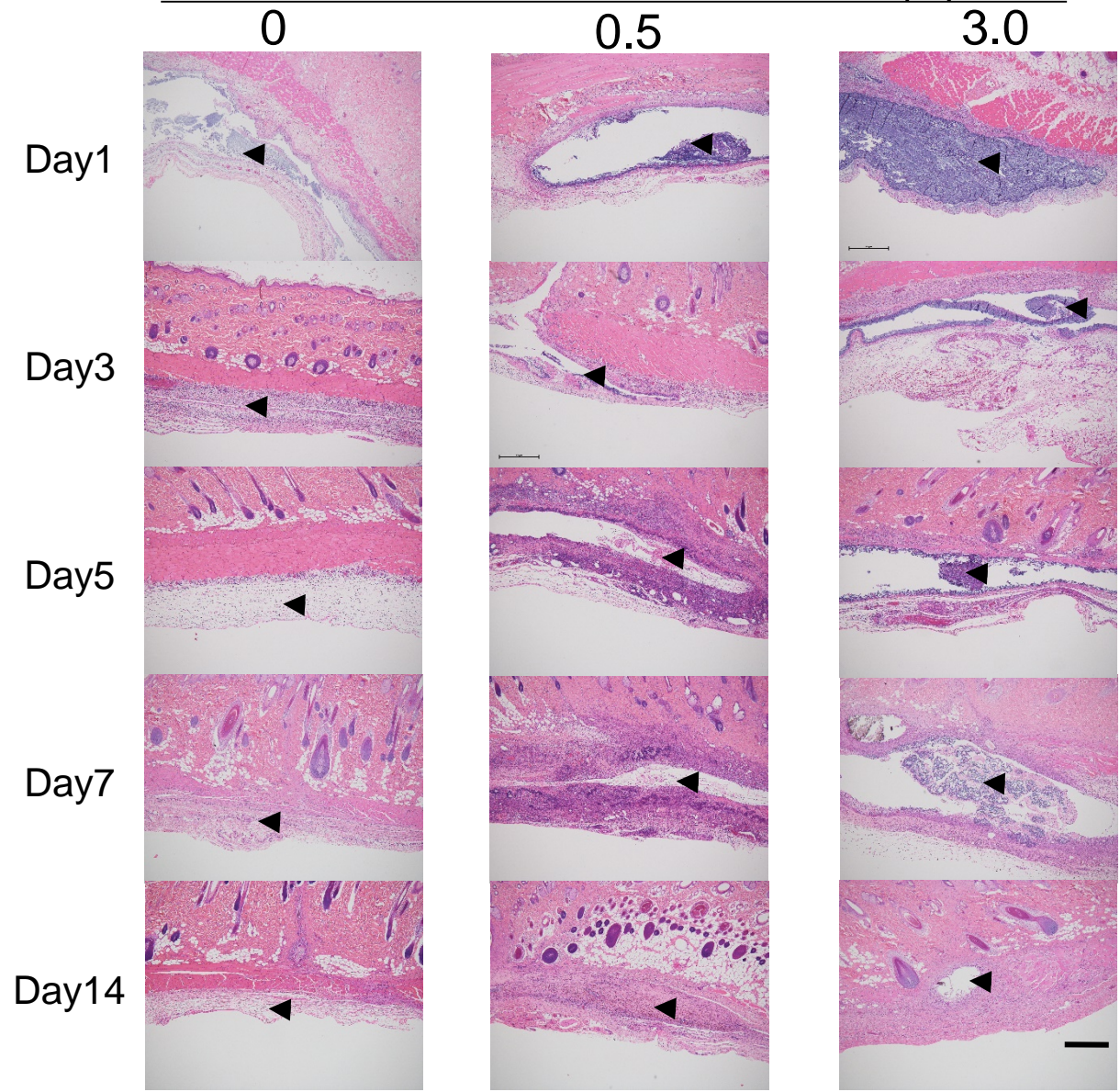
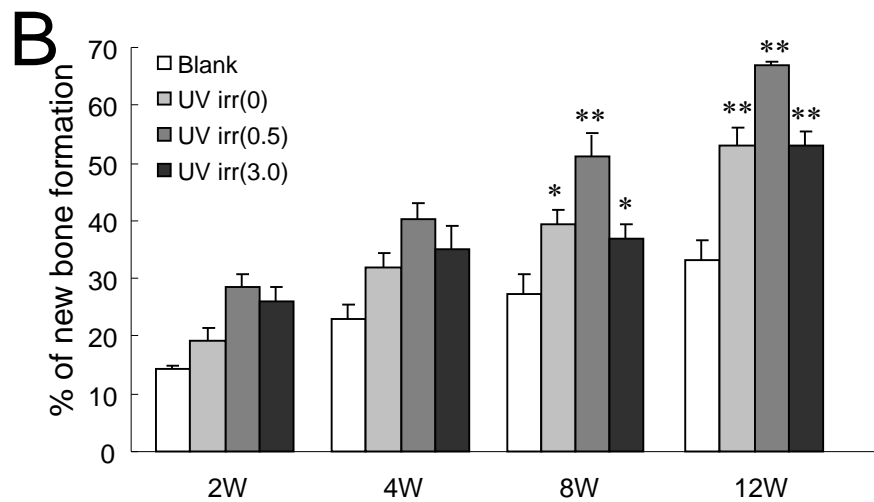
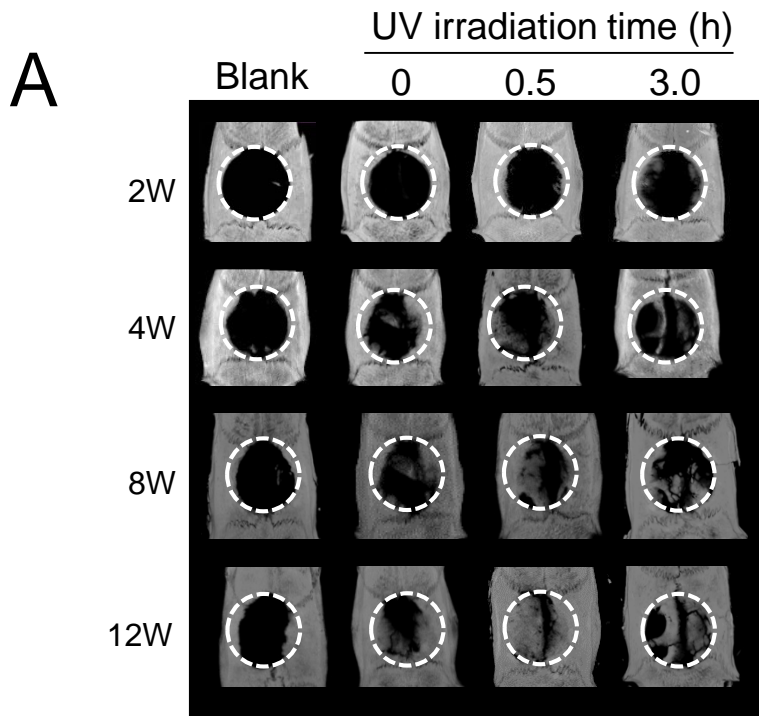


Fig. 2



C

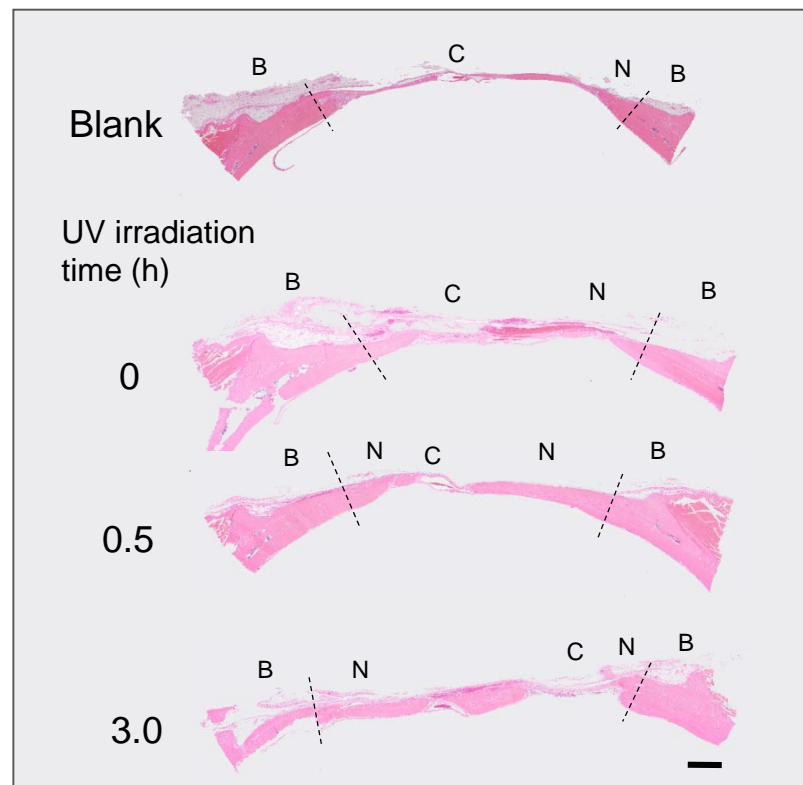


Fig. 3

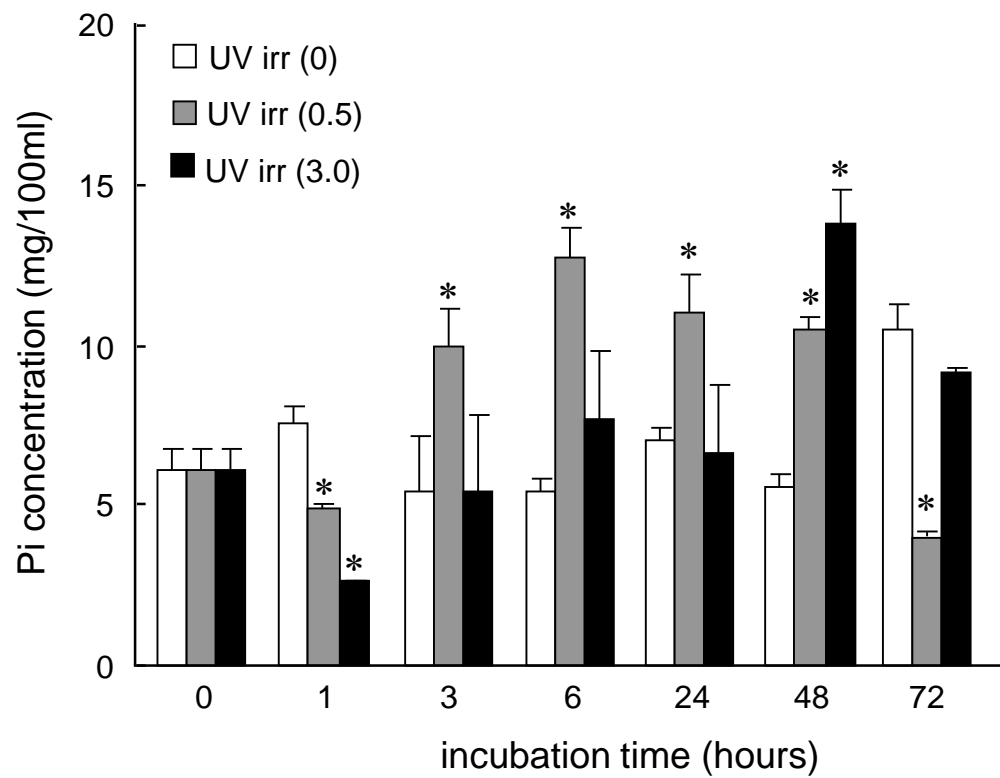
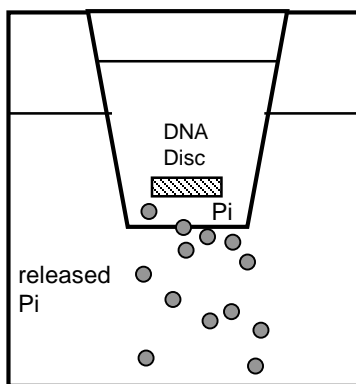


Fig. 4